

# PROCEEDINGS OF SPIE REPRINT



SPIE—The International Society for Optical Engineering

*Reprinted from*

## *Advanced Sensors and Monitors for Process Industries and the Environment*

4–5 November 1998  
Boston, Massachusetts



**Volume 3535**

# Measuring Pressure with Cavity Ring-Down Spectroscopy

Roger D. van Zee, J. Patrick Looney, & Joseph T. Hodges  
Process Measurements Division  
Chemical Science and Technology Laboratory  
National Institute of Standards and Technology  
Gaithersburg, Maryland 20899 U.S.A.

## ABSTRACT

This paper discusses recent research at NIST aimed towards the use of cavity ring-down spectroscopy as an absolute partial pressure sensor. The motivation for this work is reviewed, the concepts behind cavity ring-down spectroscopy are outlined, and recent results are summarized. The paper ends with a look at future metrological uses of this technique.

**Keywords:** cavity ring-down spectroscopy, CRDS, humidity, partial pressure, pressure, vacuum

The continual struggle for increased yield, improved quality, and greater sophistication in the electronic component and device industries has lead to an increased interest in the adverse effects of contaminants in fabrication processes. Many of the deleterious effects that trace impurities cause have been documented, and many others doubtlessly remain undiscovered. While much attention has focused on particulate contamination and remediation, the role of gaseous contamination is a growing concern. This concern has lead to new efforts to link specific gaseous contaminants to specific defects and has spurred the development of new techniques for sensing these species.

This paper discusses one aspect of this larger problem, namely, how to measure very small partial pressures. The paper starts with several examples of the effects of trace gases on manufacturing processes. Some problems associated with measuring gases at these levels using conventional instruments are given, how cavity ring-down spectroscopy might ameliorate these difficulties is discussed, and some experimental results illustrating this method's capabilities are presented. The paper closes with a look at future implementations of this technology.

## 1. THE PROBLEMS AND CHALLENGES THAT CONTAMINANTS PRESENT

Water, carbon monoxide, and molecular hydrogen are amongst the most important and ubiquitous contaminants in vacuum systems, and all of these species can alter film growth. For example, it is well established that the morphology of aluminum thin films grown by vapor deposition is altered and the film resistivity increased when water is incorporated into the film.<sup>1,2</sup> At a deposition rate of  $0.5 \text{ nm s}^{-1}$ – $1.5 \text{ nm s}^{-1}$ , these effects become appreciable at a water pressure<sup>†</sup> as low as  $10^{-5}$  Pa. In a similar vein, it has recently been discovered that trace levels of carbon monoxide alter the morphology of homoepitaxial layers of platinum on Pt[111]. These experiments demonstrated<sup>3</sup> that carbon monoxide preferentially adsorbed onto step-atoms, even when dosed to a 0.001 monolayer coverage. This adsorption forced growth at other crystal features. When the crystal was not dosed—and carbon monoxide sources were eliminated from the vacuum system—growth took place at the sites where the carbon monoxide had been adsorbed! Even the hydrogen that outgasses from the stainless steel used to construct a vacuum system can be the source of contamination for certain thin film processes. For example, in low-temperature epitaxial growth on silicon, hydrogen causes epitaxy loss at certain layer thicknesses, and the epitaxial thickness decreases in proportion to the hydrogen level.<sup>4</sup> While trace gases often have unwanted effects, this is not always so. Experiments have shown that under some conditions water and molecular oxygen produced the desirable effect of decreasing photoresist etch rates of aluminum films.<sup>5</sup> Under other etch conditions, partial pressures of these same gases as high as 0.05 % had no effect on the etch rate.

We have just seen how trace gases can alter a growth or etching process, but contaminants can react too. A good example comes

---

<sup>†</sup>A temperature of 295 K was assumed for all pressure/number density conversions.

from the manufacture of photonic devices such as light emitting diodes, lasers, and photodetectors. Typically, high purity semiconductor layers are made by thermal decomposition of gases, including phosphine, arsine, silane, and ammonia, followed by epitaxial growth at the substrate. Under these conditions, trace quantities of water or oxygen can decompose, generating oxygen complexes that become incorporated deep in the semiconductor band gap. This gives a device with degraded luminescent efficiency<sup>6</sup> and reduced minority carrier lifetime.<sup>7</sup> The relatively high chemical affinity between oxygen and aluminum makes this problem especially important in photonic devices that utilize aluminum containing compounds such as AlInGaP or AlGaAs.<sup>8,9</sup> Many photonic devices are also grown using organometallic compounds such as trimethyl gallium and trimethyl aluminum. These materials also react readily with water and oxygen to form alkoxides, which contain highly reactive hydroxyl functional groups.

Measuring source gas purity with the requisite sensitivity and accuracy—and in real time—provides the data needed to quantify the effects of impurities and can help a manufacturer adapt to changing process conditions. Devices such as electrolytic sensors, mechanical microbalances, and capacitance sensors have been developed as in-line sensors for detecting water vapor at partial pressures between 1 Pa – 10  $\mu$ Pa. These devices do not directly measure gas phase water concentration. Rather, they measure changes in the surface or bulk properties induced by moisture. Moreover, these measurements have poor precision and suffer from irreproducibility and long-term drift. Consequently, these devices require frequent recalibration. Often, “standard” humidity generators, based upon flow dilution and empirical water vapor diffusion rates, are used for calibration of these instruments. These industrial standards themselves, however, suffer from large uncertainties and are not currently traceable to primary methods of measurement of water vapor concentration.

While ideally no unwanted gas would be in a process environment, realistically *in situ* sensors are needed. The most common of these sensors is the residual gas analyzer. Tilford and co-workers<sup>10,11</sup> have studied how these analyzers respond to different gas mixtures, and their work has revealed a number of problems. One example is given in Fig. 1. Here the measured ion current from the  $m/z=40$  peak ( $\text{Ar}^+$ ) is plotted as a function of time for three partial pressure analyzers. Initially, an equilibrium argon pressure was established in the test chamber. Then water vapor was introduced and removed. Problems are immediately apparent. First, the  $m/z=40$  ion current changes when water is in the system. Second, each instrument has a different, time-dependent response, which includes a slow recovery and the evolution of a new, post-exposure sensitivity to argon. Similar problems are observed for other gas mixtures. It is believed that ion space charge in the ionization region causes the initial signal rise, and that the gradual decrease and recovery of the sensitivity are probably caused by redox reactions changing the surface conductivity of the quadrupole mass filter rods. Reducing the emission current and/or increasing the ion energy can mitigate the first effect, although this may result in reduced sensitivity and/or degraded resolution.<sup>11</sup> The second, time-dependent effects may be endemic to the operation of mass spectrometers in the presence of reactive gases. These performance characteristics obviously increase the difficulties of real-time gas monitoring and process control with commercial residual gas analyzers.

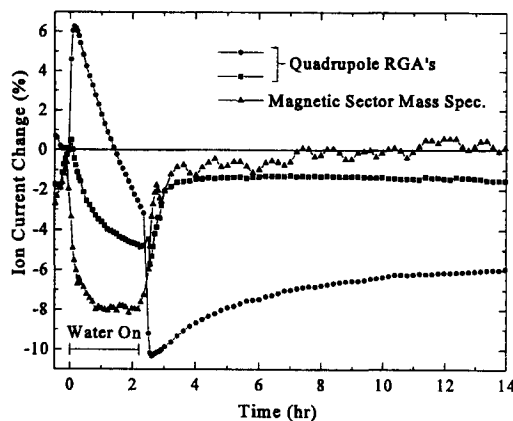


Fig. 1.  $\text{Ar}^+$  signal ( $m/z=40$ ) in three residual gas analyzers after exposure to water. A pressure of 0.44 mPa of argon was established in the chamber and maintained throughout the experiment. Starting at  $t=0$ , 0.13 mPa of water was introduced for 2.2 hr. Ref. 10 & 11. Data courtesy of S. A. Tison & C. R. Tilford.

The previous paragraph discussed how the sensitivity of a residual gas analyzer could vary with gas mixtures. Even more serious, however, these instruments, even when properly used, can be a source of unwanted gases. Figure 2 gives an illustrative example. The pressure of carbon monoxide in a baked, all-metal ultrahigh-vacuum system was monitored using resonance-enhanced, multiphoton-ionization mass spectrometry.<sup>12</sup> The test chamber was equipped with three vacuum monitoring instruments, two hot cathode ion gauges and a quadrupole mass spectrometer. At the start, all three instruments were operating. As time progressed, the instruments were turned off sequentially. As is clear, the background carbon monoxide levels correlated with the operation of each instrument, an unambiguous indication that these instruments were generating carbon monoxide. Similar experiments

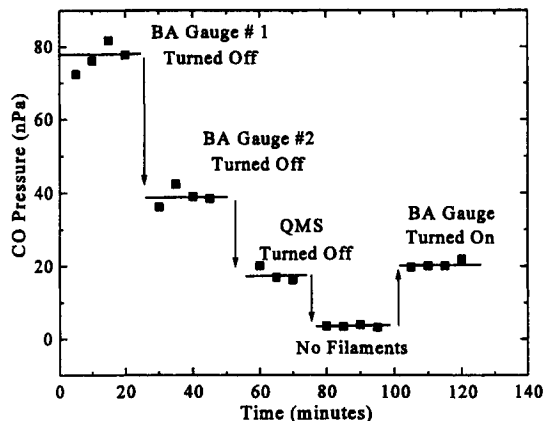


Fig. 2. Carbon monoxide pressure in an ultrahigh vacuum chamber measured by multiphoton ionization mass spectrometry. BA Gauge = Bayard-Alpert Ionization Gauge; QMS = Quadrupole Mass Spectrometer.

and water mass. However, it is impractical to measure a water partial pressure less than 0.5 Pa, because, at a minimum, weeks are required to make the measurement. Humidity levels as low as 0.1 mPa are produced at NIST using thermodynamic-based standard generators. Although these generators are highly stable and reproducible,<sup>20</sup> their accuracy is limited by a fractional uncertainty of  $\geq 2\%$  in the vapor pressure of ice<sup>21,22</sup> for temperatures below  $-50\text{ }^{\circ}\text{C}$ .

The foregoing issues have motivated the search for new ways to measure partial pressure. This new approach must be able to monitor specific molecular species, independent of the ambient pressure or gas composition, and must have at least the sensitivity and precision of existing technology. Ideally, it would be non-perturbative and have a fast response time. Finally, this new approach should be a first principles approach, that is, be rooted in rigorous physical theory, thereby having uncertainties that can be identified, measured, and controlled.

## 2. CAVITY RING-DOWN SPECTROSCOPY

Spectroscopic measurements have many of the desired properties outlined above. Kirchhoff and Bunsen recognized this in an 1860 paper in which they marveled at the incredible sensitivity and species selectivity of their crude prism spectrometer.<sup>23</sup> The unique spectra of individual molecules makes it possible to detect specific molecular species. No reactive elements need to be introduced into the sample, thereby making the method non-perturbative. Numerous spectra have been catalogued, and absorption is a well understood phenomenon, making these methods rigorously understandable. The advent of lasers renewed interest in sensors based on light/matter interactions and led to many publications and new patents, if few commercial products. The ongoing simplification and extension of optical technology is, perhaps, leading to the long held vision of a simple optical sensor. One of the most promising approaches for such a device is cavity ring-down spectroscopy (CRDS). Originally conceived of shortly after the invention of the laser,<sup>24</sup> this method was rediscovered a decade ago<sup>25</sup> and reinvigorated by technological advances that made very high reflectivity mirrors possible.<sup>26</sup> CRDS now enjoys widespread use, and it is potentially a good solution for the measurement problems discussed earlier.

Before going further, let us take a look at the cavity ring-down method. A typical cavity ring-down experiment is shown conceptually in Fig. 3. The central element of the experiment is the ring-down cavity, which is made of two highly reflective mirrors (reflectivity,  $R > 0.9999$ , typically). A pulsed light source is used to "excite" this cavity. In the excitation process, only a small amount of the incident light enters the cavity and becomes "trapped" in the cavity because of the high reflectivity of the mirrors. This trapped light circulates in and slowly leaks out of the ring-down cavity. When certain combinations of the radii of curvature of the mirrors

demonstrated that the amount of carbon monoxide generated by a hot filament gauge also depended linearly on the concentration of other common vacuum impurities, including molecular hydrogen and molecular oxygen.<sup>13</sup> Evidence suggests that such instruments are the sole source of carbon oxides and hydrocarbons in all-metal, ultrahigh-vacuum systems.<sup>14,15</sup>

Making standards-grade measurements of partial pressures for reactive gases is also a challenging task. The best pressure standard at NIST, the ultrasonic interferometric mercury manometer,<sup>16</sup> cannot be used with reactive gases and only works for pressures down to  $\sim 1\text{ Pa}$ . Below that pressure, orifice-flow standards are used. These standards consist of a large vacuum chamber through which gas flows at a known rate, thereby generating a known pressure.<sup>17</sup> While these standards work well down to  $1\text{ }\mu\text{Pa}$  for inert gases such as the noble gases, nitrogen or sulfur hexafluoride, if these standards were to be used with a gas that absorbs to the chamber walls, the large vacuum systems at the core of these standards would require extended periods of passivation.<sup>18</sup> All humidity standards at NIST are at present traceable to a gravimetric hygrometer.<sup>19</sup> This standard separates water vapor from a carrier gas by flowing the mixture through a desiccant, enabling independent measurement of the dry gas volume

and cavity length are used, a single resonance of the cavity can be excited by the incident light. In this case, the decay of the optical field inside and exiting the cavity is a simple exponential decay. The time dependence of the measured signal,  $S$ , will be<sup>27-29</sup>

$$S(t) = S(t=0) \text{Exp}(-t/\tau) + S_{bl} , \quad (1)$$

where,  $t=0$  is the time origin,  $\tau$  is the ring-down time, and  $S_{bl}$  represents a background signal level. For an empty cavity of length  $\ell$  and mirrors of reflectivity  $R$ , the ring-down time will be

$$\tau_{empty} = \frac{\ell}{c(1-R)} . \quad (2)$$

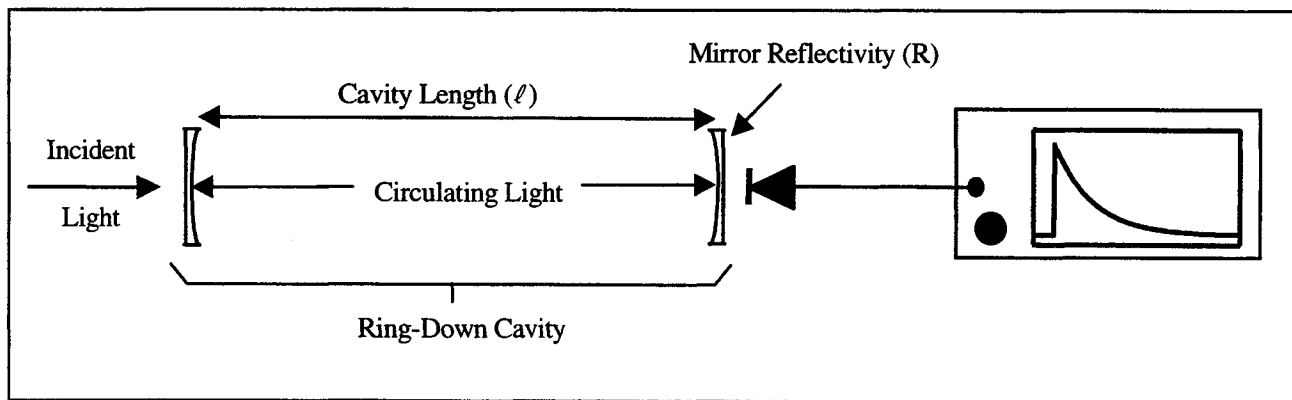


Fig. 3. A schematic representation of a typical cavity ring-down experiment.

If the cavity is filled with a gas, then light can be lost by absorption as well as through the mirrors. The losses vary as a function of frequency,  $\nu$ , across an absorption feature, and the ring-down time is given by<sup>28,30</sup>

$$\tau(\nu) = \frac{\ell}{c[(1-R) + \alpha(\nu)\ell]} . \quad (3)$$

The absorptivity,  $\alpha(\nu)$ , represents how much light the gas absorbs per unit distance.<sup>31</sup> This quantity varies across an absorption profile and is the product of the absorbing species number density,  $n$ , and the cross-section,  $\sigma(\nu)$ . Thus, by substituting the expression for absorptivity into Eq. 3, it is seen that number density is

$$n = \frac{\tau_{empty} - \tau(\nu)}{\sigma(\nu) c \tau_{empty} \tau(\nu)} . \quad (4)$$

This formula shows that if the cross-section is known, then measuring a number density using CRDS just entails measuring two ring-down times. Finally, a number density can easily be converted to a pressure using the ideal gas law, if the temperature is also known.

CRDS has some inherent advantages over conventional absorption measurements. First, the method is impervious to the ambient, since all measurements take place in the ring-down cavity itself. No reference signal that would propagate through a control sample or the atmosphere is needed. This advantage is particularly useful when measuring water, since room air typically contains about 1 kPa of water. Second, this technique eliminates sensitivity to amplitude and phase noise of the source laser. Since each ring-down measurement is referenced only to the initial ring-down intensity [ *i.e.*  $S(t=0)$  ], the cavity ring-down method is insensitive to amplitude fluctuations in the intensity of the light source. Similarly, sensitivity to phase noise in the incident field is removed because the ring-down cavity acts as a high finesse ( $>10^4$ , typically) Fabry-Pérot interferometer or étalon, and therefore has very narrow

resonances (kHz). Consequently, the cavity selects only that portion of the incident light spectrum which overlaps the narrow frequency interval of the cavity resonances. This selection removes any adverse effect that a frequency chirp, for example, might have on the signal of a conventional absorbance measurement. Third, as already noted, only two ring-down times need to be measured to determine a number density if the cross section is known. This simplicity is unique amongst spectroscopic methods. Fourth, the single-mode implementation of CRDS presented above eliminates the need to deconvolute the laser spectrum from the absorption spectrum,<sup>32</sup> a manipulation that compromises sensitivity and is needed in conventional implementations of CRDS.<sup>25</sup>

Cavity ring-down spectroscopy is competitive with alternative spectroscopic approaches as well. Perhaps the most important reason is the high sensitivity that can be achieved. As we shall discuss in more detail later, CRDS has a practical detection limit  $\leq 10^{-13}$  cm<sup>-1</sup>. For the absorption cross sections of water, this absorptivity would correspond to a number density of  $\sim 10^4$  molecules cm<sup>-3</sup>; excellent sensitivity. This level of sensitivity compares favorably to those achieved with alternative absorption techniques, such as frequency-modulation spectroscopy<sup>33</sup> or the so-called noise-immune, cavity-enhanced method.<sup>34</sup> Further, this performance simply outstrips what can be realized when a multipass absorption cell is used in conjunction with a continuous-wave laser<sup>35</sup> or an infrared spectrophotometer.<sup>36</sup> Another advantage is that a ring-down cavity hold over a multipass cell is that it is comparatively compact, since the sample size in the transverse direction is determined by the sub-millimeter scale beam diameter. Consequently, a relatively small gas volume can be sampled and some spatial resolution is possible. Finally, the ease with which these experiment can be understood—and implemented—is another critical advantage that CRDS offers. Equation 1 is derived from first principles. By contrast, although the analysis of a frequency-modulated spectroscopy experiment is equally rigorous,<sup>33</sup> it is relatively convoluted compared to the analysis required of CRDS signals. For some techniques, such as photoacoustic spectroscopy,<sup>37</sup> intracavity-laser absorption spectroscopy,<sup>38</sup> or multiphoton ionization spectroscopy,<sup>12</sup> the measured signal evolves through a series of complicated processes, thereby introducing extra layers of interpretation and approximation in the analysis, not to mention extra opportunities for error in the measurement.

### 3. THE NIST CRDS EXPERIMENTAL APPARATUS

Two essential components are required for the best ring-down measurements.<sup>28,29</sup> First, a ring-down cavity with a very stable length is needed. This requirement is important since the resonant frequency of the cavity depends on the cavity's length. Second, a laser with a stable central frequency and a good spatial profile is required. The former requirement arises because it is important to keep the laser and the cavity resonant, and the latter requirement facilitates coupling of the incident light into the ring-down cavity. In the paragraphs below, an experimental apparatus fulfilling requirements and the data acquisition process are discussed.

Length, and hence frequency, stabilization of the ring-down cavity was achieved by building the ring-down cavity from a nickel:iron alloy, chosen for its comparatively low coefficient of thermal expansion ( $10^{-6}$  K<sup>-1</sup>), and housing the entire assembly in a temperature-controlled enclosure. A cross section of this cavity is shown in Fig. 4. The ring-down cavity was formed by two 20 cm radius of curvature dielectric mirrors, which were separated by  $\sim 10.5$  cm. The overall cavity length was varied using a piezoelectric element. The cavity was sealed with o-rings and evacuated by a drag pump that was backed by a diaphragm pump. The base pressure in the cavity was  $\sim 100$  mPa, and the leak rate was  $\sim 3$  Pa hr<sup>-1</sup>. The diurnal temperature variations were  $\pm 10$  mK, and the variations during an hour were  $\pm 2$  mK, corresponding to frequency shifts of about 4 MHz and 0.8 MHz, respectively, in the resonance frequency of the ring-down cavity.

An optical parametric oscillator (OPO) generated the light for the experiments reported in this paper. A schematic of this OPO is shown in Fig. 5. The frequency doubled output (532 nm) of an injection-seeded Nd<sup>3+</sup>:YAG laser operated at 10 Hz pumped the oscillator. The oscillator itself consisted of a three mirror ring and a 1 cm-long, type-II-cut potassium titanyl phosphate crystal. The geometric length of the resonator was nominally 12 cm. An external-cavity diode laser seeded the oscillator, and the oscillator was locked to its seed laser. The frequency stability of the OPO was derived from a transfer cavity that was locked to a frequency stabilized He:Ne laser.<sup>39</sup> The transfer cavity was a confocal étalon constructed using dielectric mirrors of modest finesse at the Nd<sup>3+</sup>:YAG fundamental wavelength (1.064  $\mu$ m), the OPO seed wavelength (760 nm), and the He:Ne laser neon 3s<sub>2</sub>-2p<sub>4</sub> transition wavelength (632.8 nm). The geometric length of the transfer cavity was 30 cm. The transfer cavity derived its stability from locking to the He:Ne laser, and the seed lasers, in turn, were stabilized by locking to the transfer cavity. The OPO was tuned by varying the frequency of an acousto-optic modulator, through which the OPO seed laser double-passed before being directed into the transfer cavity. When pumped at a fluence of  $\sim 2$  J cm<sup>-2</sup>, the OPO generated  $\sim 1$  mJ of signal light in a pulse  $\sim 4.5$  ns in duration and with a full-width at half-maximum spectral bandwidth of  $\sim 115$  MHz. The stability in the central frequency was measured to be  $\sim 3$  MHz.

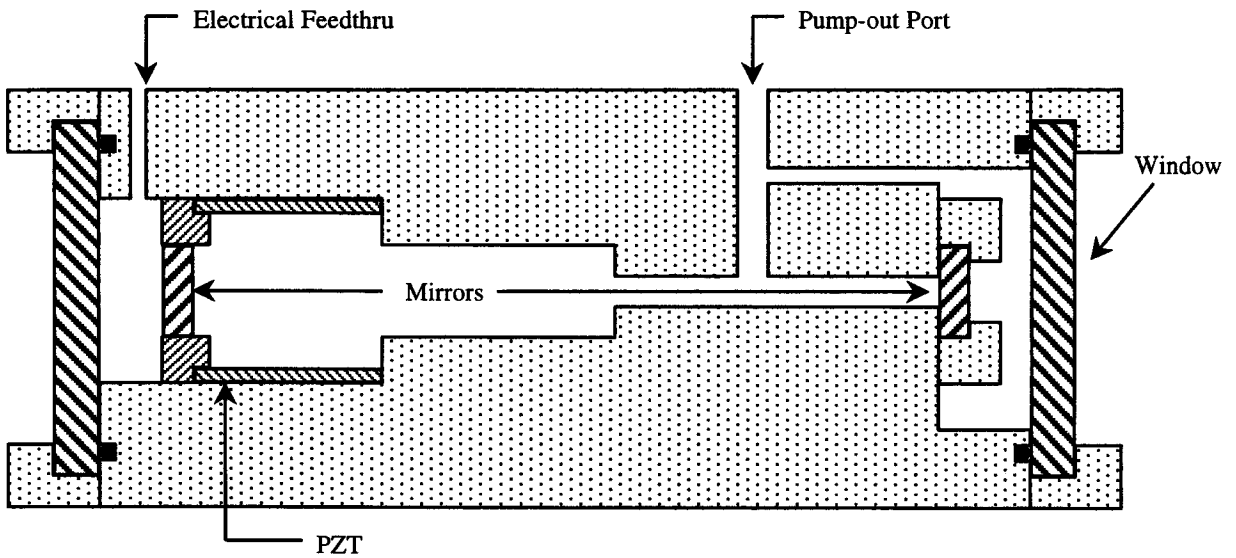


Fig. 4. A cross sectional view of the ring-down cavity used in these experiments.

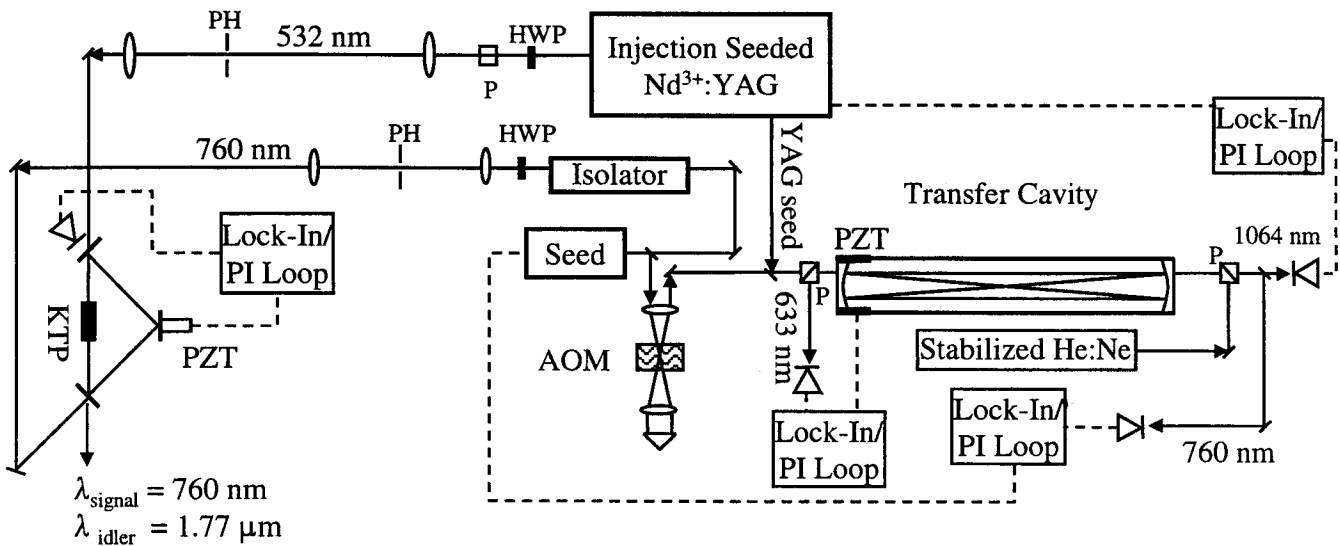


Fig. 5. A schematic layout of the optical parametric oscillator used in these experiments. PH-pin hole, HWP-half waveplate; AOM -acousto-optic modulator; PZT-piezoelectric, P-cube polarizer.

A silicon photodiode with a transimpedance amplifier served as the detector. The signal from this detector was terminated into  $50\ \Omega$  and sampled by an analog-to-digital converter at 10 ns intervals. Each individual ring-down trace was downloaded from the digitizer to a personal computer for analysis. The average value of the baseline signal preceding the excitation was computed and subtracted from the decay signal. After taking the natural logarithm of the baseline-corrected signal, the decay time constant and initial signal levels were extracted from a weighted, least-squares linear fit to the data. Each point was weighted by the reciprocal of the variance, which, after accounting for the logarithmic transformation, is

$$\frac{1}{\sigma_i^2} = \left( \frac{h\nu \mathcal{R} G}{S_i \Delta t} + \frac{\sigma_{tech}^2}{S_i^2} \right)^{-1} \quad (5)$$

The first of the two terms in parentheses accounts for the shot-noise of the exiting flux (where  $h\nu$  is the photon energy;  $\mathcal{R}$  the photodiode responsivity;  $G$  the transimpedance gain of the amplifier;  $S_i$  the voltage of the  $i$ -th sample;  $\Delta t$  the time interval between digitized samples). The second term accounts for all the technical noise in the system, including the dark current noise, noise in the amplifier, and the uncertainty associated with the finite vertical voltage resolution of the digitizer. The technical noise variance was taken to be the variance in the baseline preceding the ring-down trace.

#### 4. CAVITY RING-DOWN MEASUREMENTS

A typical ring-down signal and the residuals to an exponential fit are shown in Fig 6. This empty cavity signal has a ring-down time of  $8.534\ \mu\text{s}$ . This time constant corresponds to a loss of  $41.11 \times 10^{-6}$  per pass. The random uncertainty in this measurement was assessed by measuring and fitting five hundred ring-down curves. A histogram of these extracted ring-down times is exhibited in Fig. 7. The measurements follow a normal distribution, as shown by the fit. The fractional uncertainty about the mean (the standard deviation divided by the mean,  $\sigma_\tau / \bar{\tau}$ ) is  $3.3 \times 10^{-4}$ . This uncertainty is about a factor of eight away from the theoretical, shot-noise limit of the measured photon flux (cf. Eq. 5).

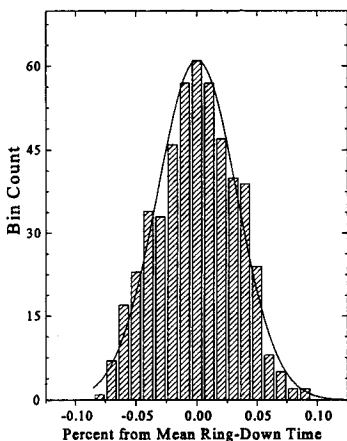


Fig. 7. A histogram of the extracted ring-down times for a set of 500 measurements. A fit to a normal distribution is also shown (—).

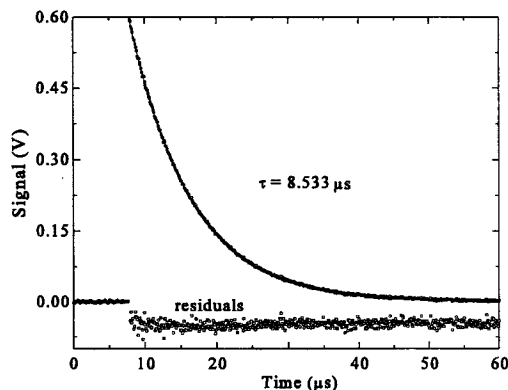


Fig. 6. A typical ring-down curve. The residuals from a fit to Eq. 1 are shown, magnified five times and displaced.

To illustrate how the pressure could be extracted from a ring-down spectrum, the spectrum of the  ${}^{\text{P}}\text{Q}(9)$  line of the A-band of molecular oxygen has been measured. This transition was

chosen because the cross section has been carefully measured and because it is “triply forbidden” (*i.e.* the cross section is very small,<sup>40</sup>  $\sim 2.5 \times 10^{22}\ \text{cm}^2$  on resonance). Thus, a small absorptivity, which is the quantity actually measured in absorption experiments, can be generated at comparatively high gas pressures. This small absorptivity will correspond to smaller number densities for more strongly absorbing molecules.

The scan data are shown in Fig. 8. Here the spectrum was plotted in the ordinary manner, that is, losses as a function of frequency. This spectrum is the average of four consecutive scans. On an individual scan, each point was based on the average of the ring-down times extracted from ten laser shots. For the data shown here, the extracted number density is  $4.827 \times 10^{16}\ \text{cm}^{-3}$  (1.966 hPa). This value is 1.4 % lower than the value calculated using the ideal gas law and the measured sample pressure and temperature,  $4.889 \times 10^{16}\ \text{cm}^{-3}$ . Several factors can account for this difference. First, extracting an accurate number density depends on having an accurate cross section. The published values used here<sup>40</sup> have an estimated precision of  $\sim 1.5\%$ , and



in previous experiments we have noted an  $\sim 1\%$  difference between published values and our data. Furthermore, the pressure gauge used in these experiments could have a systematic measurement error<sup>41</sup> between  $0.5\% - 1\%$ . A second point to be noted is the precision with which these measurements can be made. Propagating the uncertainty through Eq. 4 shows that the minimum measurable absorptivity is

$$\alpha_{\min} = \frac{\sigma_{\alpha}}{\sqrt{N}} = \sqrt{\frac{2}{N}} \frac{\sigma_{\tau}}{\tau^2 c}, \quad (6)$$

where  $N$  is the number of measurements of the ring-down time. Based on the statistics observed reported above, this equation would give  $\alpha_{\min} \sim 5 \times 10^{-10} \text{ cm}^{-1}$  for a set of ring-down measurements taken during a one second interval using the laser system described here. For oxygen probed through these bands, this corresponds to a pressure of  $< 1 \text{ cPa}$ . It must be remembered, however, that these experiments actually measure absorptivity and not number density directly (cf. Eq. 4). As illustrated in Fig. 9, this minimum detectable absorptivity would correspond to a number density of  $3 \times 10^8 \text{ molecules cm}^{-3}$  for water probed at  $\hat{\nu} = 7100 \text{ cm}^{-1}$ ,  $2 \times 10^7 \text{ molecules cm}^{-3}$  for carbon monoxide at  $\hat{\nu} = 2174 \text{ cm}^{-1}$ , and  $5 \times 10^5 \text{ molecules cm}^{-3}$  for

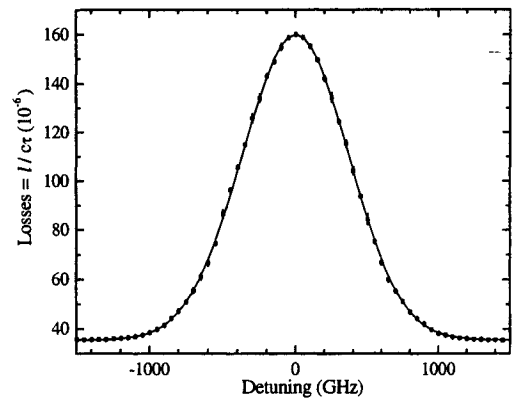


Fig. 8. A spectrum of the  ${}^9\text{Q}(9)$  line of the  ${}^{16}\text{O}_2$  A-band.

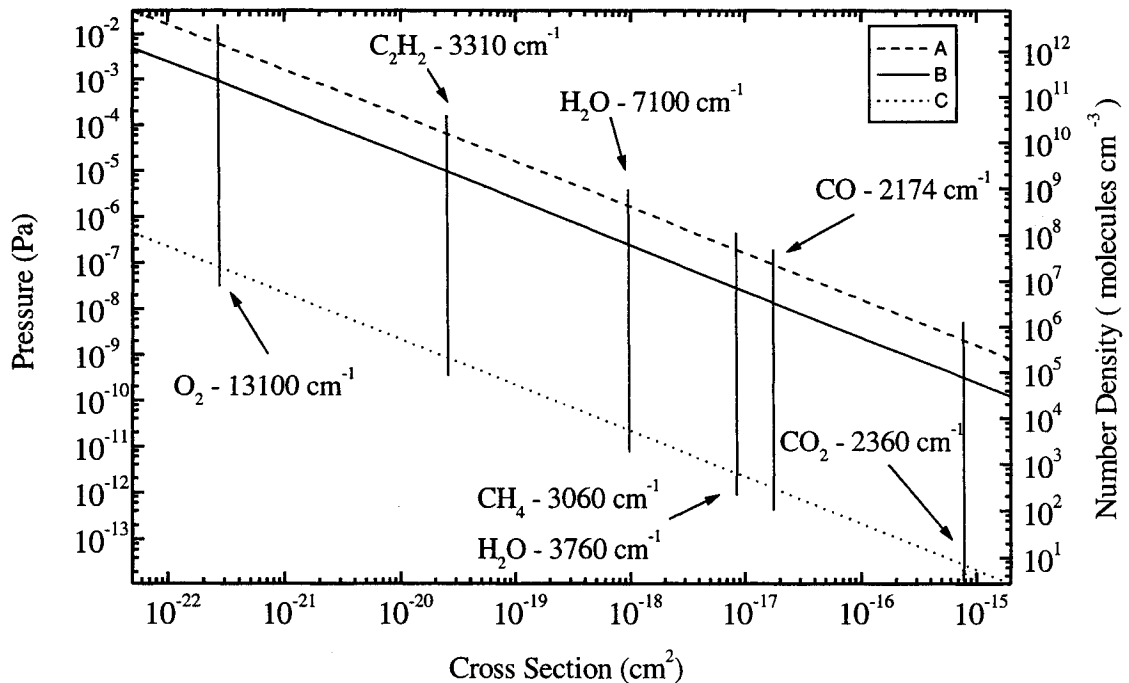


Fig. 9. A plot of the lowest number density measurable during a one second measurement interval as a function of cross section for three sensitivities: A—as demonstrated in this paper, 10 cm-long cavity, mirror reflectivity of 0.99996,  $\sim 1.5 \text{ nW}$  of average laser power exiting the ring-down cavity; B—shot-noise limit for these experiments; C—shot-noise limit for a 1 m-long cavity, mirror reflectivity of 0.99999, and  $100 \mu\text{W}$  of average laser power exiting the ring-down cavity. The cross sections of select molecules, along with the transition frequencies, are shown with vertical lines.

carbon dioxide probed at  $\tilde{\nu}=2360\text{ cm}^{-1}$ . CRDS measurements at infrared wavelengths ( $100\text{ cm}^{-1} - 10000\text{ cm}^{-1}$ ) will use detectors and mirrors different from those used in these experiments. Accordingly, it must be acknowledged that extending CRDS measurements to infrared wavelengths at the precision reported here might be hindered by technical impediments, such as detector linearity, detector quantum efficiency and noise, the dynamic range and bandwidth of the digitizer, electronic noise in the digitizer circuits, or some other unforeseen nonideality.

## 5. POSSIBILITIES

With the measurement precision and sensitivity that has been demonstrated here, it is worthwhile to think about how this method might be used in the future. One can imagine possibilities for the method as a process sensor, in standards characterization, and in high precision spectroscopy.

Since its inception, there has been considerable interest in using CRDS as a process sensor, a challenge both researchers and entrepreneurs are pursuing. One of the important, perhaps the most important, factor for making this technique a commercially viable tool is to obtain the required sensitivity with a compact device. The research reported here, in which absorptivities that correspond to water number densities of  $10^9\text{ molecules cm}^{-3}$  were measured with a 10 cm-long ring-down cell, moves toward that goal. Work has begun here to build and attach a CRDS instrument to a vapor deposition system in which laser diodes are grown, in order to correlate device defects with specific impurities. While the industrial demands for simplicity and ruggedness are still beyond where the technology now stands, demonstrating the usefulness of these spectroscopic tools in the laboratory may lead to viable instruments tomorrow.

Cavity ring-down spectroscopy might be a viable pressure standard in select pressure regimes. Current pressure standards at NIST have fractional uncertainties of  $10^{-2} - 10^{-3}$  between  $1\text{ }\mu\text{Pa} - 10\text{ Pa}$  and  $10^{-3} - 10^{-5}$  in the range  $10\text{ Pa} - 5\text{ kPa}$ . At the shot-noise limit, the uncertainties associated with a ring-down measurement are competitive with the uncertainties of these present standards. For such a standard to be realized, the line strength must be known with the requisite precision and accuracy. For example, the quadrupole lines of molecular hydrogen have line strengths<sup>††</sup> [ $10^{-29} - 10^{-26}\text{ cm}^{-1} (\text{molecule cm}^{-2})^{-1}$ ] that make these transitions suitable for measuring pressure between  $1\text{ kPa} - 1\text{ MPa}$  at the current precision. To be a viable alternative to existing standards, however, it would be necessary to have a line strength calculated from first principles, with an accuracy  $\sim 0.001\%$ , a demand that might be difficult to meet. Alternatively, the line strength could be measured at a point where the number density is well-known. Water would be one such candidate, since at its triple point the fractional uncertainty in the vapor pressure<sup>42</sup> has been measured to be less than  $0.002\%$ . The line strength of one or more rovibrational transition of water could be measured at the triple point. This measurement would yield a line strength that could be used to measure number densities at other temperatures and pressures.

The improvements gain in metrological applications of CRDS could also benefit other areas of applied and fundamental spectroscopy. We have demonstrated<sup>43</sup> that a line strength can be measured with a random error of  $\sim 0.3\%$  using CRDS. Line strengths measured with this precision should prove valuable in certain areas, such as atmospheric modeling where numbers with this level of precision would help in studies of the energy transfer budget in the upper atmosphere. Accurate measurement of the far wings of pressure broadened lines at the precision shown here would allow detailed tests of alternative line shape theories.

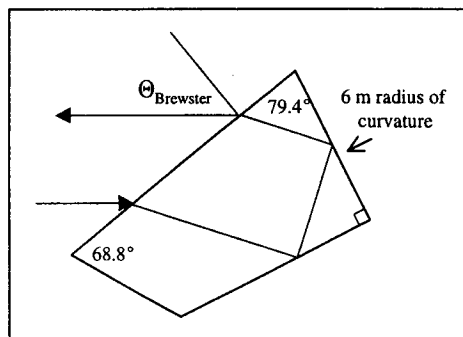


Fig. 10. Brewster's angle retro-reflector for CRDS.

If CRDS is to be used routinely as a standard or a process sensor, it will be important to simplify the system, especially the infrared laser system. Recent advances on compact optical parametric oscillators, quantum cascade lasers, and external cavity diode lasers promise to make such light sources available in the near future. The availability of mirrors is another possible obstacle, for while dielectric mirrors can in principle be made from the ultraviolet through the infrared regions, these mirrors are not readily available at all wavelengths. Along with K. K. Lehmann of Princeton University, we have begun work on an alternative to dielectric mirrors, based on a "Brewster's angle retroreflector." Half of a cavity made from these prisms is shown in Fig. 10. The prisms are adjusted so that the light circulating in the cavity strikes a prism at Brewster's angle. Light is reflected,

<sup>††</sup>Line strength =  $\int \sigma(\nu) d\nu$

twice, by total internal reflection, before being sent back towards the other prism. Light can be coupled into these cavities using photon tunneling or by turning one prism slightly away from Brewster's angle and using the Fresnel reflection from that prism face. The orientation of these prisms can be changed to accommodate, in principle, wavelengths from the ultraviolet through the infrared. Prototypes have been polished from fused silica, and, in initial tests, round trip losses of  $\sim 500 \times 10^{-6}$  per pass have been measured. These advances coupled with the many contributions of other research groups may eventually make CRDS a viable process sensor for certain applications where the cost and complexity of such a detector would be merited.

## 6. REFERENCES

1. M. J. Verkerk and W. A. M. C. Brankaert, "Effects of water on the growth of aluminium films deposited by vacuum evaporation", *Thin Solid Films* **139**, pp. 77-88 1986.
2. G. J. van der Kolk and M. J. Verkerk, "Microstructural studies of the growth of aluminum films with water contamination", *J. App. Phys.* **59**, pp. 4062-4067, 1986.
3. M. Kalf, G. Comsa, and T. Michely, "How sensitive is epitaxial growth to adsorbates?", *Phys. Rev Lett.* **81**, pp. 1255-1258, 1998.
4. D. J. Eaglesham, "Semiconductor molecular-beam epitaxy at low temperatures", *J. Appl. Phys.* **77**, pp. 3597-3617, 1995.
5. A. Glew, J. Ammenheuser, J. Riddler, and A. Johnson, "Determining the effects of trace gas impurities in semiconductor thin film processes", SEMITECH Report No. 96083175A-XFR, 1996.
6. H. Terao and H. Sunakawa, "Effects of oxygen and water vapour introduction during MOCVD growth of GaAlAs", *J. Cryst. Growth*, **68**, pp. 157-162, 1984.
7. J. C. Chen, Z. C. Huang, K. J. Lee, and R. Kanjolia, "Effects of trimethylindium on the purity of  $\text{In}_{0.5}\text{Al}_{0.5}\text{P}$  and  $\text{In}_{0.5}\text{Al}_{0.5}\text{As}$  epilayers grown by metalorganic chemical vapor deposition", *J. Electron. Mater.* **26**, pp. 361-365, 1997.
8. T.F. Kuech, R. Potemski, F. Cardone, and G. Scilla, "Quantitative oxygen measurements in OMVPE  $\text{Al}_x\text{Ga}_{1-x}\text{As}$  grown by methyl precursors", *J. Electron. Mater.* **21**, pp. 341-346, 1992.
9. M. Suzuki, K. Itaya, Y. Nishikawa, H. Sugawara, and M. Okajima, "Reduction of residual oxygen incorporation and deep levels by substrate misorientation in InGaAlP alloys", *J. Cryst. Growth*, **133**, pp. 303-308, 1993.
10. C. R. Tilford, "Characteristics of partial pressure analyzers", *Damage to Space Optics, and Properties and Characteristics of Optical Glass*, J. B. Breckinridge and A. J. Marker, eds., Proc. SPIE **1761**, pp. 119-129, 1992.
11. C. R. Tilford, "Optimizing residual gas analyzers for process monitoring", *Proc. Symp. On Process Control, Diagnostics, and Modeling in Semiconductor Manufacturing*, M. Meyyappan, D. J. Economou, and S. W. Butler, eds., **97-7**, pp. 184-191, Electrochemical Society, 1997.
12. J. P. Looney, J. E. Harrington, K. C. Smyth, T. R. O'Brian, and T. B. Lucatorto, "Measurement of CO pressures in the ultrahigh vacuum regime using resonance-enhanced multiphoton-ionization time-of-flight mass spectroscopy", *J. Vac. Sci. Technol. A*, **11**, pp. 3111-3120, 1993.
13. J. P. Looney, "Laser photoionization measurements of pressures in vacuum", *J. Vac. Soc. Jpn.* **37**, pp. 703-710, 1994.
14. J. K. Fremerey, *J. Vac. Soc. Jpn.* **37**, p. 718 ff., 1994.
15. J. R. J. Bennett and R. J. Elsey, "Anomalies in the measurement of the residual gases in a largeuhv system using a quadrupole mass analyzer", *Vacuum*, **44**, pp. 647-651, 1993.
16. C. R. Tilford, "Three and a half centuries later-the modern art of liquid-column manometry", *Metrologia*, **30**, pp. 542-552, 1993/1994 and references therein.
17. C. R. Tilford, S. Dittmann, and K. E. McCulloh, "The National Bureau of Standards primary high-vacuum standard", *J. Vac. Sci. Technol. A* **6**, pp. 2853-2859, 1988.
18. S. A. Tison and C. R. Tilford, "Low-density water vapor measurement; The NIST primary standard and instrument response", *Proc. RL/NIST Workshop on Moisture and Control for Microelectronics*, B. A. Moore and J. Carpenter, Jr. eds., NISTIR 5241, pp. 19-29, U. S. Dep't. of Commerce, 1993.
19. A. Wexler and R.W. Hyland, "The NBS standard hygrometer", NBS Monograph 73, U. S. Dep't. of Commerce, 1964.
20. G. E. Scace, D. C. Hovde, J. T. Hodges, P. H. Huang, J. A. Silver and J. R. Whetstone, "Performance of a precision low frost-point humidity generator", *Papers and Abstracts from the Third International Symposium on Humidity and Moisture*, **1**, National Physical Laboratory, pp. 180-190, 1998.
21. A. Wexler, "Vapor pressure formulation for ice", *J. Res. Natl. Bur. Stand. Sec. A* **81**, pp. 5-20, 1977.
22. J. Marti and K. Mauersberger, "A survey and new measurements of ice vapor pressure at temperatures between 170 and 250 K", *Geophys. Res. Lett.* **20**, pp. 363-366, 1993.

23. G. R. Kirchhoff and R. Bunsen, "Chemische analyse durch spectralbeobachtungen", *Poggendorfs Ann.* **110**, pp. 161-189, 1860.
24. O. E. DeLange, "Losses suffered by coherent light redirected and refocused many times in an enclosed medium", *Bell Sys. Tech. J.* **44**, pp. 283-302, 1965.
25. A. O'Keefe and D. A. G. Deacon, "Cavity ring-down optical spectrometer for absorption measurements using pulsed laser sources", *Rev. Sci. Instrum.* **59**, pp. 2544-2551, 1988.
26. G. Rempe, R. J. Thompson, H. J. Kimble, and R. Lalezari, "Measurement of ultralow losses in an optical interferometer", *Opt. Lett.* **17**, pp. 363-365, 1992.
27. P. Zalicki and R. N. Zare, "Cavity ring-down spectroscopy for quantitative absorption measurements". *J. Chem. Phys.* **102**, pp. 2708-2717, 1995.
28. K. K. Lehmann and D. Romanini, "The superposition principle and cavity ring-down spectroscopy", *J. Chem. Phys.* **105**, pp. 10263-10277, 1996.
29. J. T. Hodges, J. P. Looney, and R. D. van Zee, "Response of a ring-down cavity to an arbitrary excitation", *J. Chem. Phys.* **105**, pp.s 10278-10288, 1996.
30. J. P. Looney, J. T. Hodges, and R. D. van Zee, "Quantitative absorption measurements using cavity-ringdown spectroscopy with pulsed lasers", *Cavity Ringdown-Spectroscopy: A New Technique for Trace Absorption Measurements*, K. A. Busch and M. A. Busch eds., American Chemical Society, 1998, to appear.
31. L. A. Pugh and K. N. Rao, "Intensities from infrared spectra", *Modern Spectroscopy*, K. N. Rao, ed., **1**, pp. 165-177, Academic, 1976.
32. J. T. Hodges, J. P. Looney, and R. D. van Zee, "Laser bandwidth effects in quantitative cavity ring-down spectroscopy", *Appl. Opt.* **35**, pp. 4112-4116, 1996.
33. J. A. Silver, "Frequency-modulation spectroscopy for trace species detection: theory and comparison among experimental methods", *Appl. Opt.* **31**, pp.707-717, 1992.
34. J. Ye, L-S. Ma, J. L. Hall, "Ultrasensitive detections in atomic and molecular physics: demonstration in molecular overtone spectroscopy", *J. Opt. Soc. Am. B*, **15**, pp. 6-15, 1998.
35. R. S. Inman and J. J. F. McAndrew, "Application of tunable diode laser absorption spectroscopy to trace moisture measurements in gases", *Anal. Chem.* **66**, pp. 2471-2479, 1994.
36. B. R. Stallard, L. H. Espinoza, R. K. Rowe, M. J. Garcia, and T. M Niemczyk, "Trace water vapor detection in nitrogen and corrosive gases by FTIR spectroscopy", *J. Electrochem Soc.* **142**, pp. 2777-2782, 1995.
37. A. C. Tam, "Photothermal spectroscopy as a sensitive spectroscopic tool", *Optical Methods for Ultrasensitive Detection and Analysis*, B. L. Feary, ed., SPIE Proc. **1435**, pp. 114-127, 1991.
38. G. H. Atkinson, "High sensitivity time-resolved absorption spectroscopy by intracavity laser techniques", *Advances in chemical reaction dynamics*, P. M. Rentzepis and C. Capello, eds., NATO ASI Series C, **184**, Reidel, 1986.
39. E. Riedle, S. H. Ashworth, J. T. Farrell, Jr., and D. J. Nesbitt, "Stabilization and precise calibration of a continuous-wave difference frequency spectrometer by use of a simple transfer cavity", *Rev. Sci. Instrum.* **65**, pp.42-48, 1994.
40. K. J. Ritter and T. D. Wilkerson, "High-resolution spectroscopy of the oxygen A-band", *J. Mol. Spectrosc.* **121**, pp. 1-19, 1987.
41. A. E. Miiller and C. R. Tilford, unpublished results.
42. L. A. Guildner, D. P. Johnson, and F. E. Jones, "Vapor pressure of water at its triple point", *J. Res. Natl. Bur. Stand.* **80**, pp. 505-521, (1976).
43. J. T. Hodges, J. P. Looney, and R. D. van Zee, "Single-mode cavity ring-down spectroscopy for line shape measurements", *Proc. 14th International Conference on Spectral Line Shapes*, R. Herman, ed., AIP, 1998, to appear.